

## Appendix A

### Further numerical model parameters and results

Flamar uses a large strain fully explicit time-marching scheme (e.g., Francois et al., 2013). In the Lagrangian method, incremental displacements are added to the grid coordinates allowing the mesh to move and deform with the material. This allows for the solution of large-strain problems while using locally the small-strain formulation: on each time step the solution is obtained in local coordinates, which are then updated in a large-strain mode. The code locally solves full Newtonian equations of motion in a continuum mechanics approximation. The model uses visco-elasto-plastic rheologies based on Maxwell summation for deviatoric strain rate to simulate flow. At high confining pressure, Byerlee's law shows that maximal brittle strength is proportional to  $0.6 P$ , where  $P$  is the total pressure. Within our formulation, we model this experimental law using the cohesion of 20 MPa and the internal friction angle  $\Phi = 30^\circ$ . For viscous (ductile) behaviour the effective viscosity depends on the temperature and strain rate and the pre-exponential factor.

Length of model $x_L$	1000 km				
Amount of extension	144 km & 260 km				
Extension velocity	2 cm/yr				
Vertical resolution in the upper crust	1.2 km				
Horizontal resolution	2 km				
Temperature at the base of the lithosphere	1300 °C				
Radioactive heat production, $H_s$	$1.5 \times 10^{-9} \text{ W kg}^{-1}$				
Radiogenic production decay length, $h_r$	10 km				
Upper crustal thermal conductivity, $k_c$	$2.5 \text{ W K}^{-1} \text{ m}^{-1}$				
Lower crustal thermal conductivity, $k_c$	$2 \text{ W K}^{-1} \text{ m}^{-1}$				
Mantle thermal conductivity, $k_m$	$3.3 \text{ W K}^{-1} \text{ m}^{-1}$				
Thermal diffusivity of mantle, $\chi$	$10^{-6} \text{ m}^2 \text{ s}^{-1}$				
Specific heat, $C_p$	$1000 \text{ J K}^{-1} \text{ kg}^{-1}$				
Cohesion	20 MPa				
Byerlee's law friction angle	$30^\circ$				
Initial surface heat flow	$70 \text{ mW/m}^2$ & $68 \text{ mW/m}^2$				
Lamé elastic constants	30 GPa				
2D erosion coefficient in dry and wet climatic scenarios, $k_{ero}$	0 & 250 & 750 $\text{m}^2 \text{ yr}^{-1}$				
	Upper crust	Lower crust	Mantle lithosphere	Weak zone	Asthenosphere
Thickness (km)	20 & 24	20 & 24	95 & 112	-	315
Density, $\rho_0$ ( $\text{kg m}^{-3}$ )	2750	2900	3330	3270	3330
Power law constant, $A$ ( $\text{MPa}^{-n} \text{ s}^{-1}$ )	$6.7 \times 10^{-6}$	$6.3 \times 10^{-2}$	$7 \times 10^3$	$6.8 \times 10^3$	$7 \times 10^3$
Creep activation energy, $E$ ( $\text{kJ mol}^{-1}$ )	156	276	520	276	510

Power law constant, n	2.4	3.05	3	4	3
-----------------------	-----	------	---	---	---

**Table A.1.** Basic parameters of the five presented thermo-mechanical numerical experiments. Rheological parameters are adapted from similar numerical experiments (quartz-rich upper crust: e.g., Burov, 2007; Cloetingh et al., 2013; diabase lower crust: e.g., Francois et al., 2013; dry and wet olivine mantle: e.g., Burov and Poliakov, 2001 and Ranalli, 1995).

Horizontal model dimension		150 km × 120 km				
Horizontal model resolution		2.5 km				
Vertical resolution		variable ~1-100 m				
Water flow exponential, m		1.5				
Slope exponential, n		1.3				
External source sand/mud ratio		3/7				
<b>Sediment class</b>						
		Basement	Sand	Mud		
Grain size [mm]		4	0.25	0.0035		
Gravity-driven coefficient [km <sup>2</sup> /kyr]		0.01	0.03	0.03		
Water-driven continental coefficient [km <sup>2</sup> /kyr]		80	80	160		
Water-driven marine coefficient [km <sup>2</sup> /kyr]		0.08	0.08	0.8		
<b>Experiment</b>						
Experiment	Max. syn- and post-rift basement subsidence	Maximum erosion rate	Maximum sediment supply	Maximum long-term water discharge	Short-term / long-term discharge ratio	Along-strike Geometrical variability
M1wet	4.25 km, 2 km	300 m/Myr	9000 km <sup>3</sup> /Myr	2000 m <sup>3</sup> /s	18	no
M1dry	3.25 km, 1 km	200 m/Myr	6000 km <sup>3</sup> /Myr	1000 m <sup>3</sup> /s	12	yes
M2wet	4.25 km, 2 km	300 m/Myr	6000 km <sup>3</sup> /Myr	2000 m <sup>3</sup> /s	18	no
M2dry	3.25 km, 1 km	200 m/Myr	4000 km <sup>3</sup> /Myr	1000 m <sup>3</sup> /s	12	yes

**Table A.2.** Basic parameters of the 4 presented 3D stratigraphic forward numerical experiments. For details see methodology chapter and Granjeon (2014, 2019).

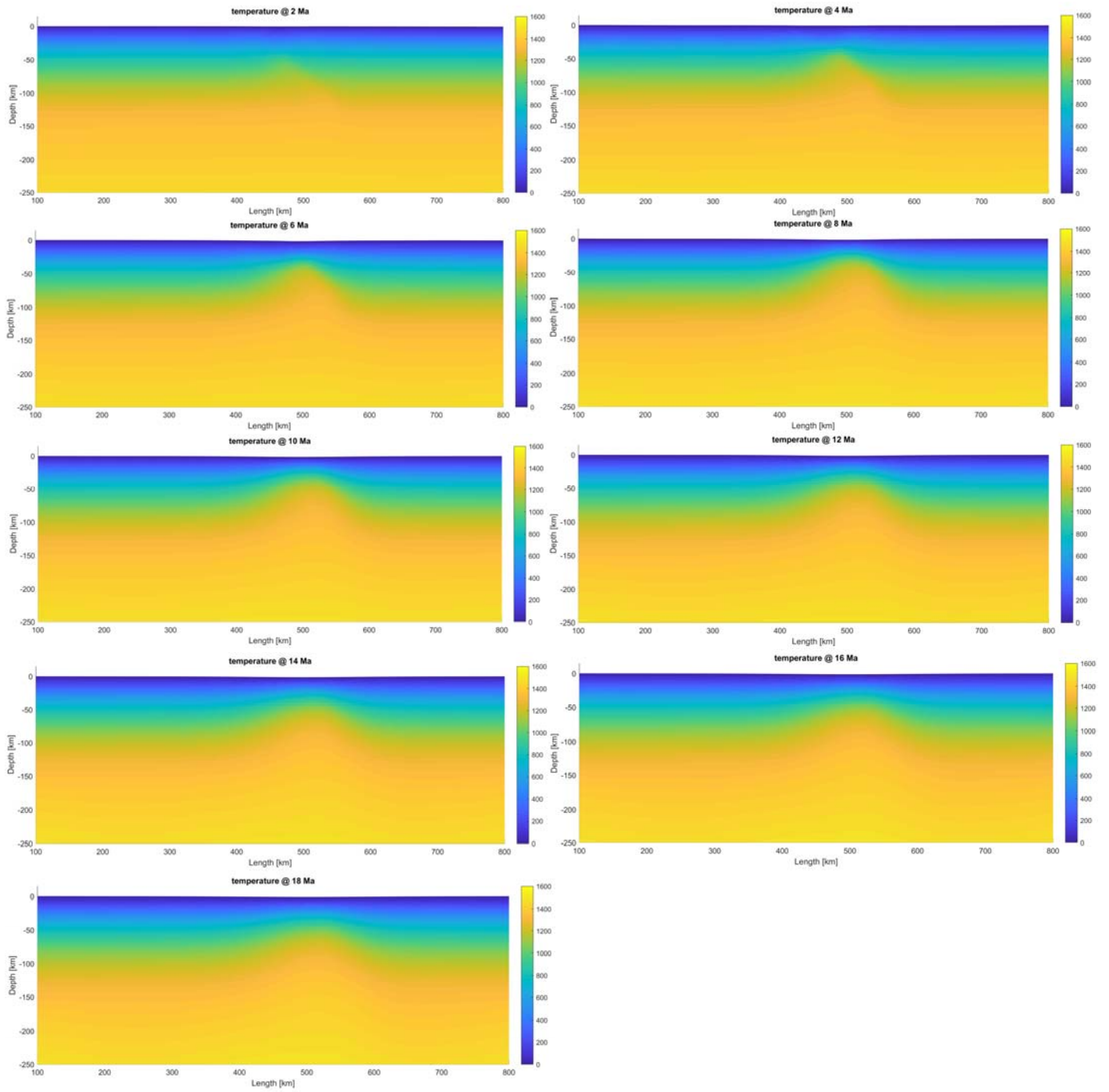


**Figure A1.** Temperature field evolution of the reference model (40 km initial crustal thickness, 750 m<sup>2</sup>yr<sup>-1</sup> erosion coefficients, syn-rift extension for 7.2 Myr).

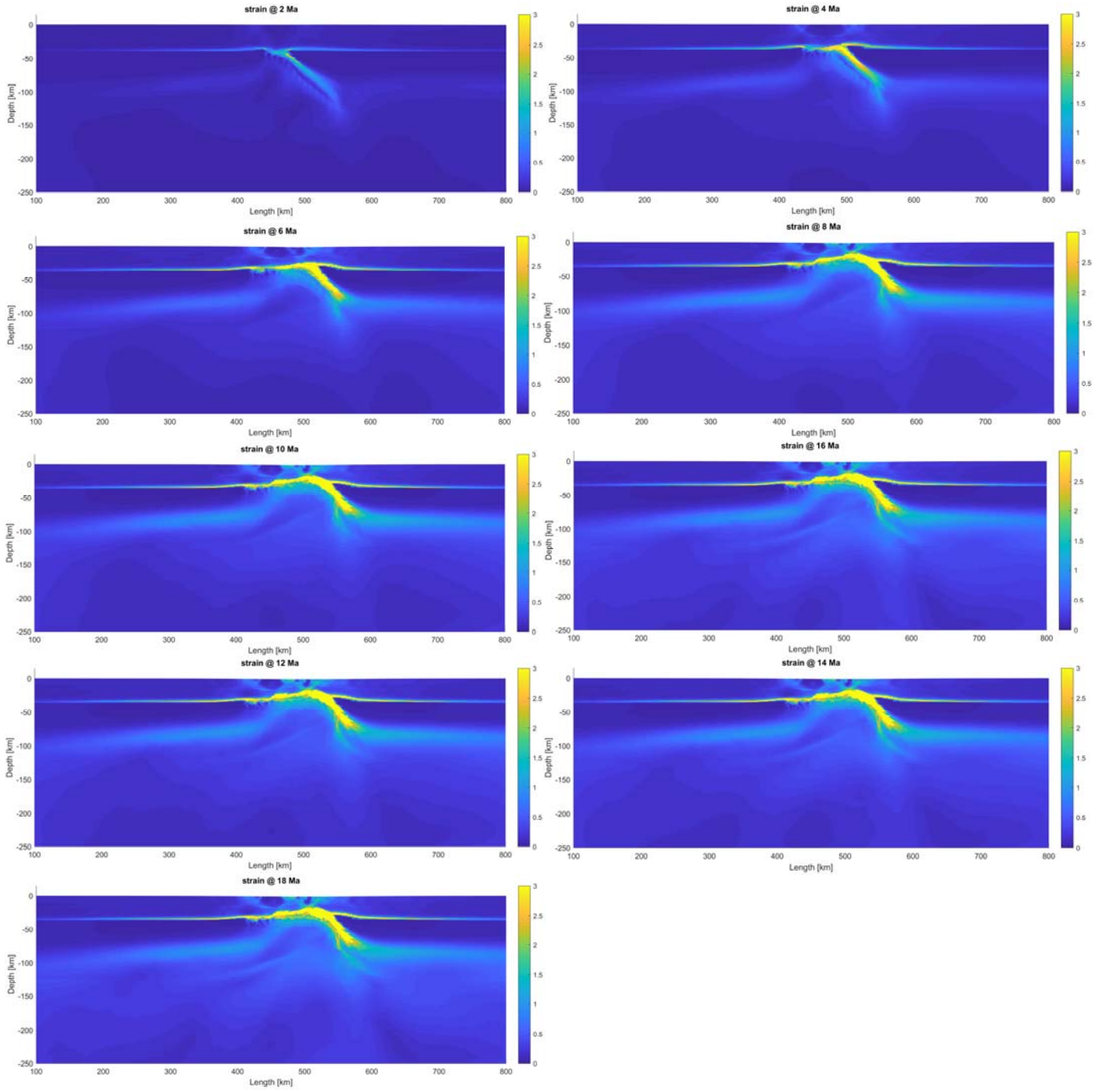


**Figure A2.** Straine field evolution of the reference model (40 km initial crustal thickness, 750 m<sup>2</sup>yr<sup>-1</sup> erosion coefficients, syn-rift extension for 7.2 Myr).

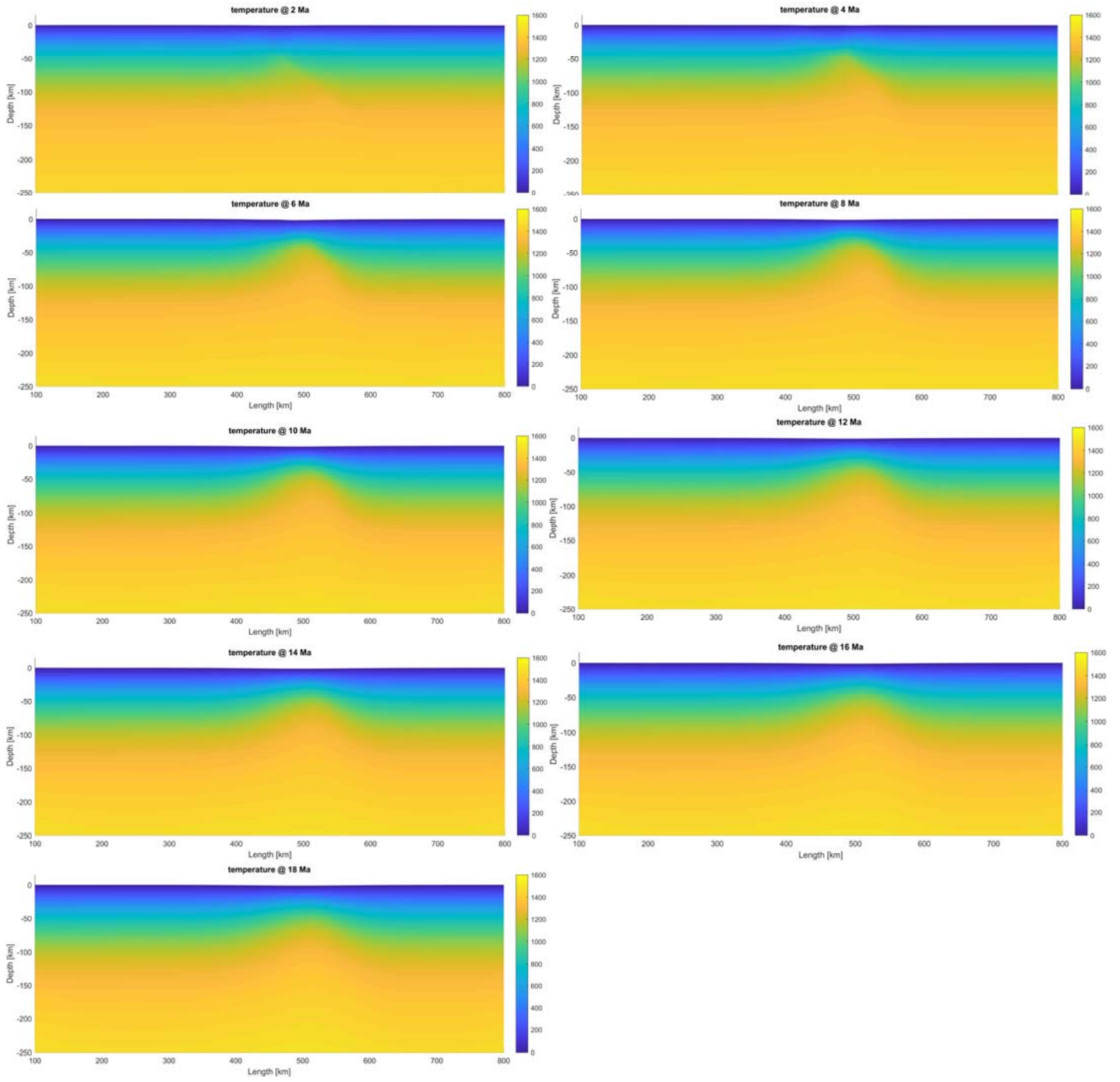


**Figure A3.** Temperature field evolution of the thermo-mechanical model with lower diffusion coefficient (40 km initial crustal thickness, 250 m<sup>2</sup>yr<sup>-1</sup> erosion coefficients, syn-rift extension for 7.2 Myr).

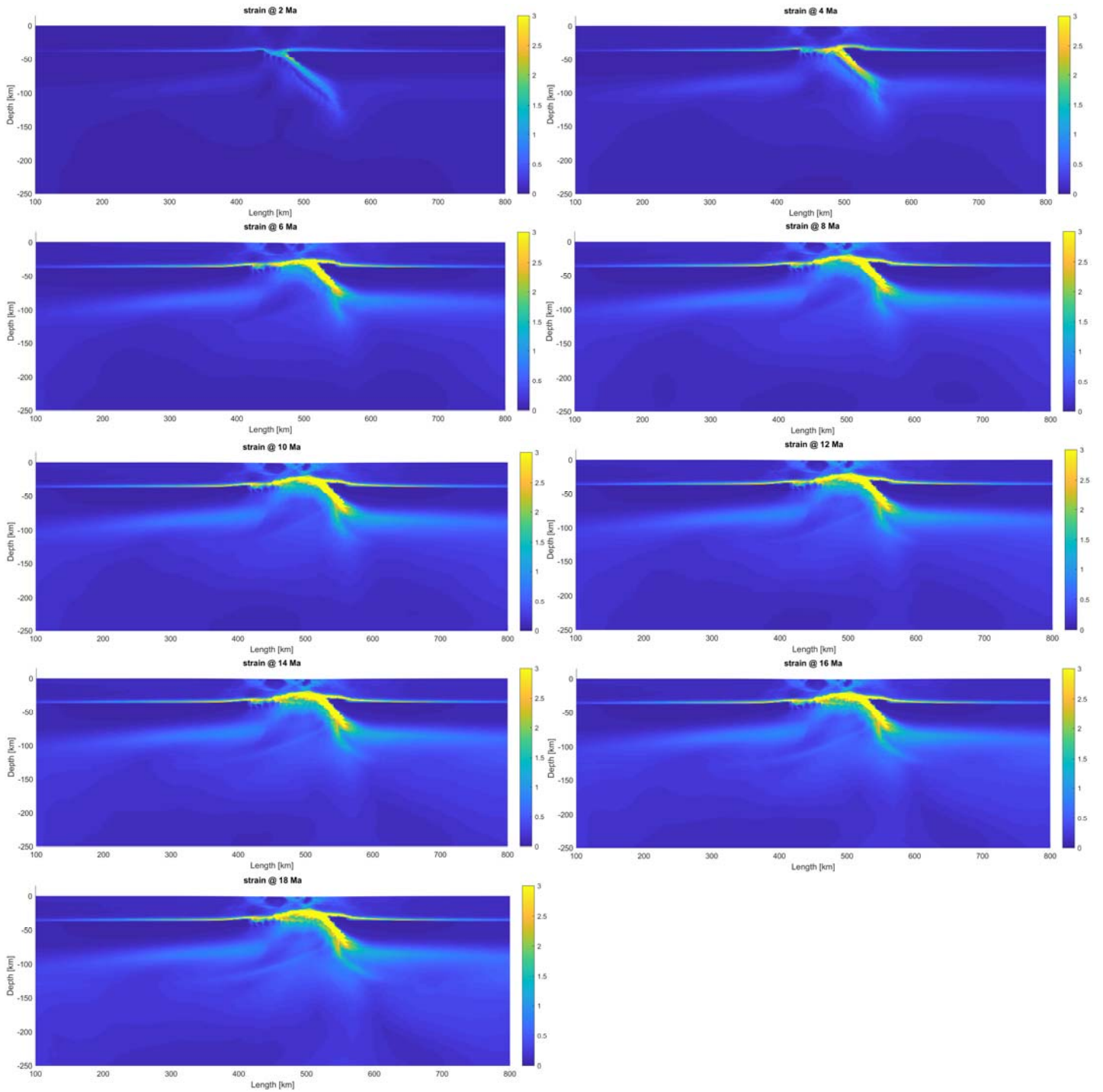


**Figure A4.** Strain field evolution of the thermo-mechanical model with lower diffusion coefficient (40 km initial crustal thickness, 250 m<sup>2</sup>yr<sup>-1</sup> erosion coefficients, syn-rift extension for 7.2 Myr).

**Figure A5.** Basement derived sediment class proposition from the reference stratigraphic experiment (model M1wet).

**Figure A6.** Basement derived sediment class proposition from the stratigraphic experiment modelM1dry.

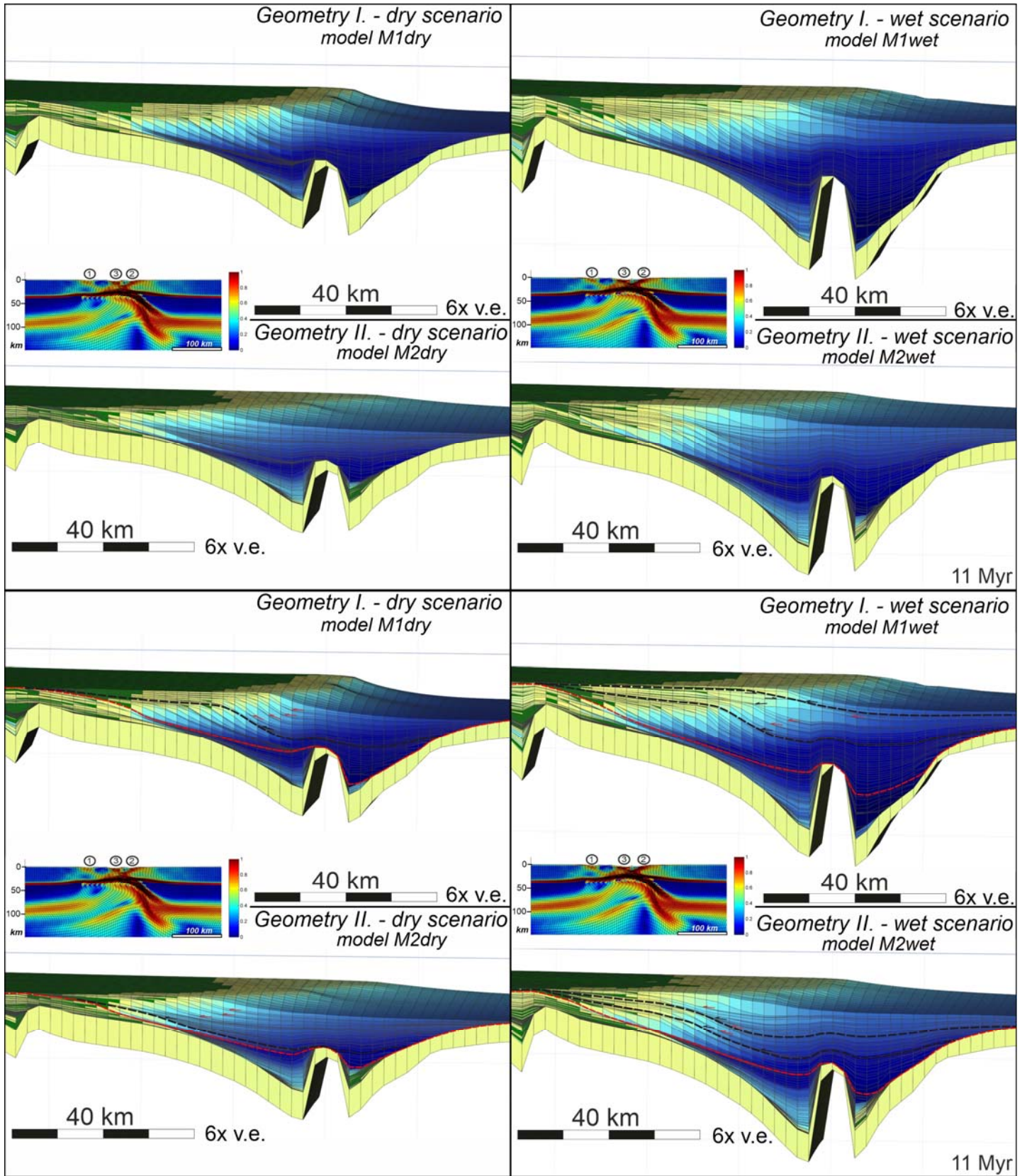


**Figure A7.** Uninterpreted and interpreted stratigraphic model results from the four experiment by DionisosFlow.



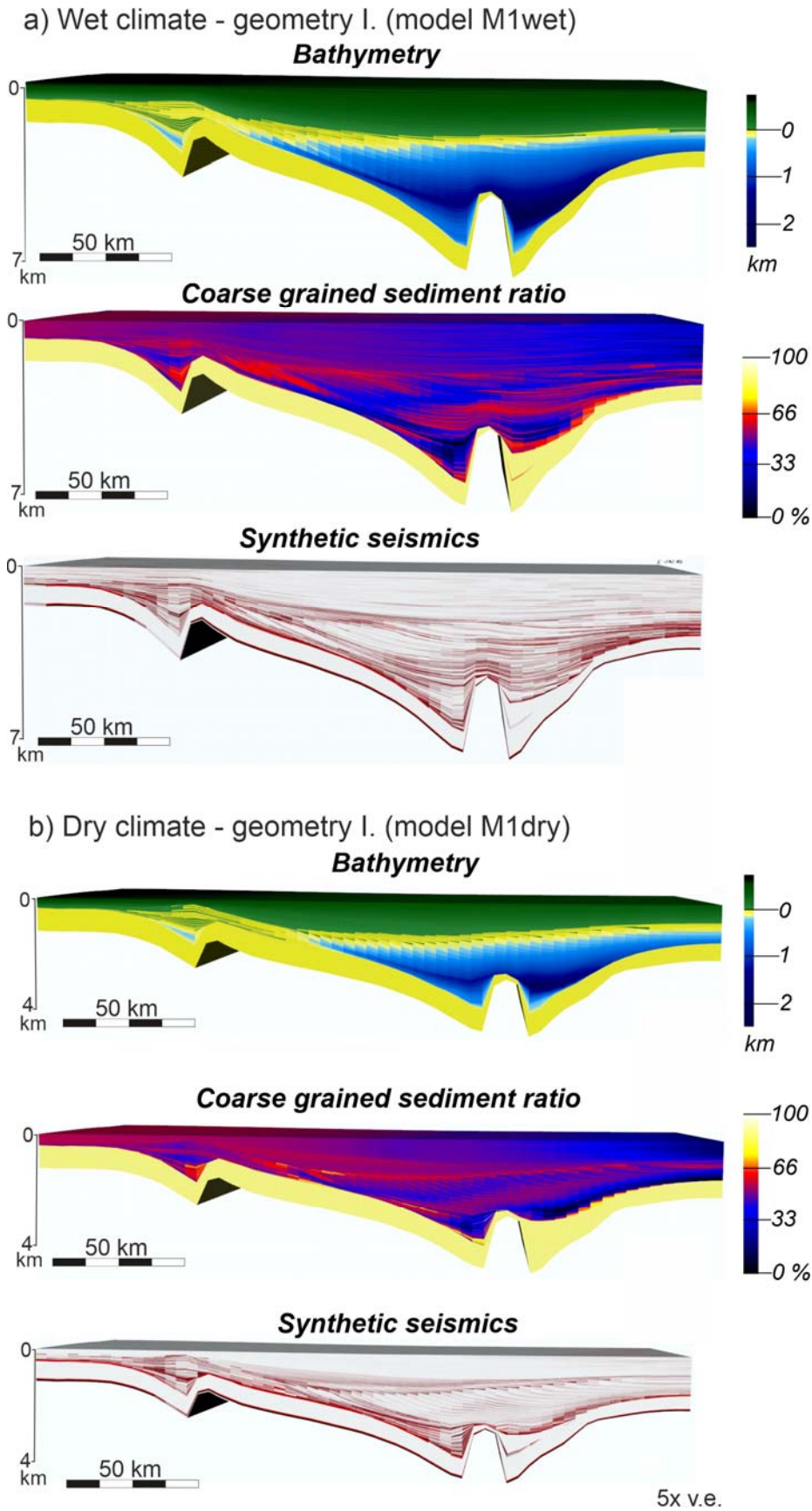
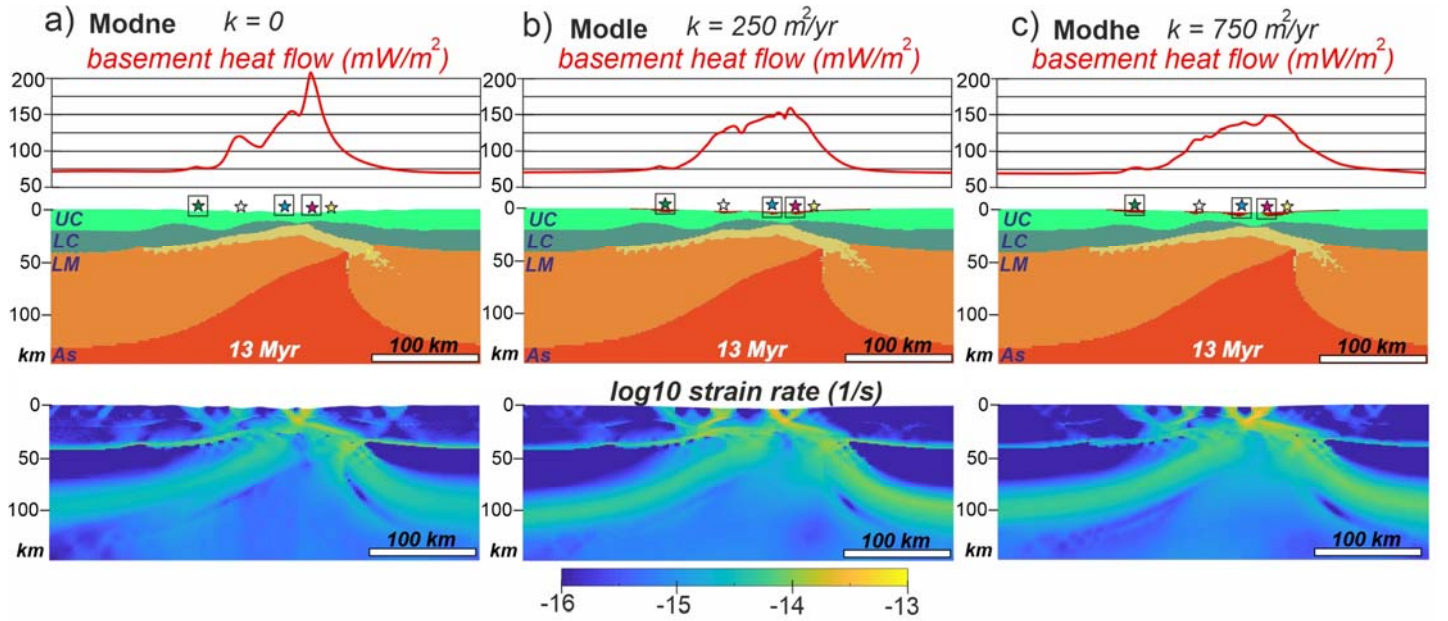


**Figure A8.** (a-b) Model results of the stratigraphic models by DionisosFlow during wet and dry climatic conditions. Coarse grained sediment ratio includes sand and basement derived cobbles together.



Increasing erosion and sedimentation coefficient

### Basement heat flow evolution ( $\text{mW/m}^2$ )

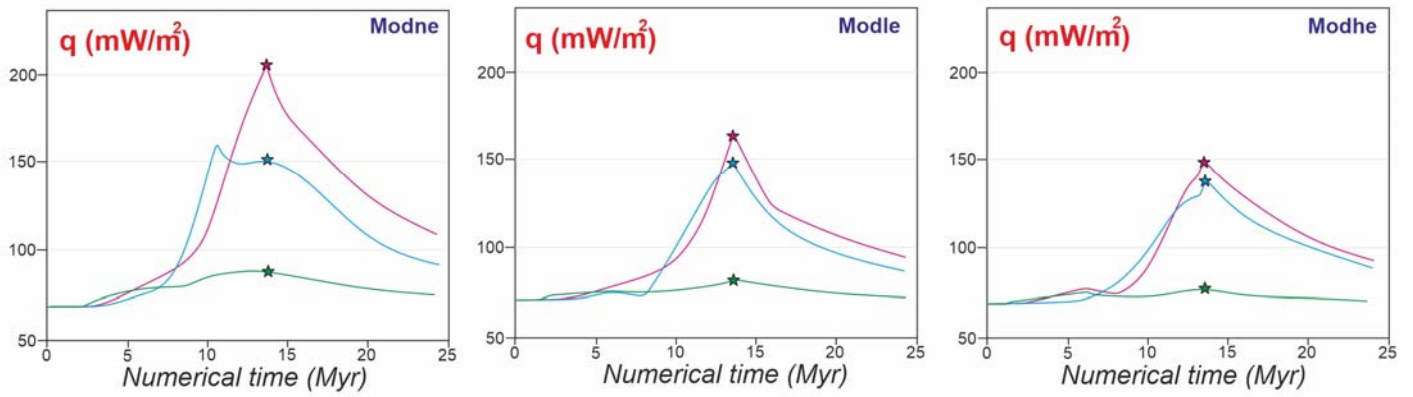


**Figure A9.** Thermal evolution of models with initially thickened crust with different erosion and sedimentation rates applied.